

## Original Research Article

# Development and *in vitro* evaluation of mucoadhesive microsphere carriers for intranasal delivery of betahistine dihydrochloride.

Bissera Pilicheva<sup>\*1</sup>, Plamen Zagorchev<sup>1</sup>, Yordanka Uzunova<sup>1</sup>, Margarita Kassarova<sup>2</sup>**\*Corresponding author:****Bissera Pilicheva**

<sup>1</sup>Department of pharmaceutical sciences, Medical University of Plovdiv, 15A Vasil Aprilov Blvd., Plovdiv, Bulgaria

<sup>2</sup>Margarita Kassarova, Department of pharmaceutical sciences, Medical University of Plovdiv, 15A Vasil Aprilov Blvd., Plovdiv, Bulgaria

**A b s t r a c t**

The aim of the present work was to formulate and evaluate betahistine-loaded chitosan microspheres intended for nasal delivery with focus on their mucoadhesive properties.

Betahistine-loaded chitosan microspheres were obtained via W/O emulsion solvent evaporation technique and were characterized for particle size, surface morphology and entrapment efficiency. FTIR spectroscopy was carried out to evaluate drug-polymer interaction and powder X-ray diffractometry was applied to investigate crystallinity transformations. Tensile studies were carried out using sheep nasal mucosa to evaluate *in vitro* mucoadhesion. Drug release into phosphate buffer saline pH 7.4 was performed and dissolution profiles of the formulations were obtained.

The results showed that the microspheres were spherical in shape having smooth surface and mean particle size of 3.82  $\mu\text{m}$  to 7.69  $\mu\text{m}$  which is appropriate for optimum deposition in the nasal cavity. The mean particle size increased when chitosan solutions with higher viscosity were used. *In vitro* mucoadhesion studies indicated that chitosan microspheres had good mucoadhesive properties and could adequately adhere to nasal mucosa. It was observed that polymer concentration enhancement led to increased mucoadhesive strength. Betahistine release studies from the microspheres showed similar and slightly increasing dissolution profiles.

According to the obtained results, betahistine-loaded chitosan microspheres prepared by solvent evaporation method proved to be capable of sustained release and could be used via nasal route as an alternative to oral administration.

**Keywords:** Ménière's syndrome, chitosan microparticles, mucoadhesion, nasal delivery, sustained release.

**Introduction**

Betahistine dihydrochloride (BET) is a histamine analogue, which is currently prescribed for the symptomatic treatment of vestibular disorders of central and peripheral origin. BET improves the microcirculation of the inner ear resulting in reduced endolymphatic pressure in the labyrinth and is, therefore widely used to relieve the symptoms associated with Ménière's syndrome [1]. The mechanism by which BET alters this microcirculation and its interaction with the histaminergic system is now well established. BET primarily acts like a partial histamine H1 receptor agonist and a more potent histamine H3 receptor antagonist. Stimulating the H1 receptors in the inner ear causes a vasodilatory effect and increased permeability in the blood vessels which results in reduced endolymphatic pressure. By blocking the histamine H3 autoreceptors, BET increases the synthesis and release of histamine in the tuberomammillary nuclei which can further increase the direct H1 agonist activity [2,3]. In clinical practice, BET is generally administered orally at a dose range 24 to 48 mg/day divided into three to four doses daily. Studies with radio-labelled BET have demonstrated a plasma half life of 3.4 hours which

necessitates frequent administration of the drug and may lead to noncompliance, especially in elderly patients [1,4].

It was thus challenging to be able to design a sustained release formulation of BET which allows a reduction of the frequency of dose while keeping drug concentration within the therapeutic range. Since the drug is freely soluble in water, specific technological approaches are required to control drug release.

Recently there has been a considerable interest in alternative routes of administration as a means of drug delivery. Among them, nasal delivery seems to be an appropriate way to prevent conditions like nausea and vomiting associated with Ménière's syndrome [5]. The widespread interest arises from the particular anatomical, physiological and histological characteristics of the nasal cavity, which provides rapid systemic drug absorption and quick onset of action. The nasal mucosa is easily accessible, highly vascularised and permeable; it provides rapid drug absorption rate and plasma drug profiles sometimes almost identical to those from intravenous injections. In addition, intranasal administration avoids the gastrointestinal and hepatic presystemic metabolism, enhancing drug bioavailability compared to gastrointestinal absorption [6,7]. The nasal delivery seems to be a favourable way



to circumvent the obstacles for blood-brain barrier allowing direct drug delivery to the central nervous system via the olfactory neurons [8].

Despite the numerous advantages, there are certain limiting factors like mucociliary clearance and enzymatic activity, that adversely affect the bioavailability of drugs and must be considered when developing a nasal formulation [9]. To overcome the problem with the low bioavailability of drugs administered via nasal route, different approaches have been studied. The use of mucoadhesive polymers has proven to be effective in providing an intimate contact with the mucosa and thereby, prolonging the residence time of drug formulations in the nasal cavity, resulting in improved nasal drug absorption. Mucoadhesion is generally achieved with the use of polymers; various mucoadhesive polymers such as gelatin, chitosan, cellulose derivatives, hyaluronic acid, starch, polyacrylic acids (eg. carbopol, polymethyl methacrylate) in different forms have been studied for the mucosal delivery of small molecules and macromolecular drugs [10].

A growing interest towards the development of polymeric carriers as a means of drug delivery has been noticed recently. Microspheres constitute an important part of these particulate drug delivery systems by virtue of their small size and efficient carrier capacity; coupling of mucoadhesive properties of polymers to microparticulate systems has additional advantages [11]. Mucoadhesive microspheres form a gel-like layer, which is cleared slowly from the nasal cavity. The prolonged residence time at the application site contributes to improved therapeutic performance of drugs namely prolonged drug release and a reduction in frequency of drug administration. Thus patient comfort and compliance are improved. Another benefit is the protection of the encapsulated drug from hazardous conditions and enhance drug stability [12].

Chitosan microspheres have received considerable attention as nasal drug delivery systems [13]. Chitosan, being biodegradable, biocompatible, non-toxic and bioadhesive polymer is a suitable excipient for use in biomedical and pharmaceutical formulations [14]. Chitosan is a cationic polysaccharide, derived by the deacetylation of chitin. Chitosan is positively charged due to its amino groups and able to interact strongly with the negatively charged mucus layer of the nasal epithelium [15]. This is to provide a longer contact time for drug transport across the nasal membrane, before the formulation is cleared by the mucociliary

clearance mechanism. In addition, chitosan has been shown to increase the paracellular transport of polar drugs by transiently opening the tight junctions between the epithelial cells [16].

In the present study chitosan microspheres intended for nasal delivery of BET were prepared by emulsification solvent-evaporation technique. The influence of different formulation variables, namely, chitosan concentration and drug-polymer ratio on the production yield, particle size, drug entrapment efficiency and *in vitro* mucoadhesion was investigated. Additionally, *in vitro* drug release from the chitosan microspheres was studied.

## Materials and Methods

Bethahistine dihydrochloride, chitosan (from shrimp shells, low viscosity, degree of deacetylation >75%), sorbitan monooleate 80 (Span 80) and petroleum ether were purchased from Sigma-Aldrich Chemie GmbH (Taufkirchen, Germany). All other reagents and solvents were of analytical grade and were used as provided.

### Preparation of chitosan microspheres

Chitosan microspheres were prepared by single emulsion/solvent evaporation technique using liquid paraffine as external phase. Briefly, chitosan was dissolved in deionized water containing 2% v/v acetic acid. Accurately weighed amount of BET was added to the polymer solution by continuously stirring until a homogeneous solution was obtained. To form a single W/O emulsion, drug-polymer solutions were slowly added dropwise to 100 ml preheated liquid paraffine containing 0.5% w/v Span 80 as an emulsifying agent at a constant stirring rate of 1100 rpm for 3.5 hours using a two blade stirrer ES (Velp Scientifica, Usmate, Italy). The temperature was maintained at 65°C throughout the process which helps in evaporation of the aqueous acidic phase and solidification of the microspheres. The hardened microspheres were separated by vacuum filtration and washed several times with petroleum ether to remove oil. Finally, microspheres were air dried for 24 h and then stored in vacuum desiccator for further use. To study the influence of different formulation variables on chitosan microspheres, four batches of formulations, labeled M1 - M4 were prepared by varying BET and chitosan concentrations and drug/polymer ratio as given in Table 1.

Table 1. Composition and physicochemical properties of BET loaded microspheres.

Formulation code	Drug concentration, %	Polymer concentration, %	Drug/polymer ratio	Yield (% ± SD)*	Entrapment efficiency (% ± SD)**	Mean particle size (m ± SD)**
M1	1	1	1:1	68.46 ± 4.98	69.37 ± 0.91	3.82 ± 0.14
M2	1	1.5	1:1.5	73.33 ± 6.67	93.02 ± 0.98	4.49 ± 0.24
M3	1	2	1:2	76.57 ± 6.44	93.85 ± 2.51	4.52 ± 0.33
M4	2	2	1:1	84.23 ± 6.73	98.27 ± 0.73	7.69 ± 0.33

\*n=5; \*\*n=3



## Microsphere characterization

### Production yield, drug content and incorporation efficiency

The production yields of microspheres of various batches were calculated using the weight of finally dried microspheres (W1) with respect to the initial total quantity of the drug and polymer used (W2). Production yields were calculated as per the formula mentioned below, and reported in Table 1.

$$\% \text{ Production Yield} = W1/W2 \times 100$$

The actual drug content of all the formulations was determined spectrophotometrically. BET- loaded microspheres were dispersed in 20 ml 2 % v/v aqueous acetic acid solution by agitation in ultrasonicator (Siel UST7.8-200, Gabrovo, Bulgaria) for 30 minutes to dissolve the polymer and extract the drug. After filtration, drug concentration was determined after proper dilution using an Ultrospec 3300 pro UV/Visible Spectrophotometer (Biochrom Ltd., Cambridge, UK) at a wavelength of 261 nm. The Drug Entrapment Efficiency (DEE) was calculated according to the following equation:

$$\text{DEE \%} = (\text{Actual drug content} / \text{Theoretical drug content}) \times 100$$

The drug entrapment efficiency for the formulations M1 to M4 is reported in Table 1.

### Particle size analysis

All batches of microspheres were studied for shape and size using optical microscope (Eclipse 80i, Nikon Engineering Co., Ltd., Japan) equipped with a camera (DS-Qi1) and computer controlled image analysis software (NIS-Elements, Nikon, Japan). At least one hundred microspheres were measured randomly and the average particle size was determined using the Edmondson's equation:

$$D_{\text{mean}} = \sum nd / \sum n,$$

where where n= number of microspheres observed and d=mean size range.

### Morphological examination

Scanning Electron Microscopy (Philips SEM 515, Eindhoven, The Netherlands) was used to examine the shape and surface morphology of the microsphere formulations. The samples were loaded on a copper sample holder and sputter coated with carbon followed by gold using vacuum evaporator (BH30). The images were recorded at 25 kV acceleration voltage using various magnifications.

### FTIR spectrophotometry

In order to evaluate the integrity and compatibility of the drug/polymer formulations, FTIR spectra were obtained. The spectra of betahistine (Fig. 3a), BET-free (placebo) particles (Fig. 3b) and model systems (Fig. 3c) were recorded on Nicolet Avatar 330 FTIR spectrometer (64 scans, 4 nm resolution, spectral range

4000-400  $\text{cm}^{-1}$ ) as spectra of transmittance and converted as absorption spectra with EZ Omnic software. The samples were prepared by KBr pellet method.

### Thermal analysis

Differential thermal analysis and thermogravimetric analysis were performed on pure drug, chitosan, placebo and drug-loaded microspheres and the results are illustrated in Figure 4.

A Stanton Redcroft TG-DTA simultaneous thermal analyser STA 1500 was used in the measurements, and a heating rate of  $10^\circ\text{C min}^{-1}$  in an argon atmosphere over a temperature range of 10 C to 450 C was applied.

### Powder X-ray diffraction (XRD) studies

X-ray diffraction studies were carried out using powder X-ray diffractometer (D2 Phaser, Bruker AXS GmbH, Karlsruhe, Germany) to get the idea of the crystallinity. The samples were irradiated with monochromatised CuK radiation and analyzed between from 4 to 60 ( $2\theta$ ), applying 30 kV, 10 mA. Powder X-ray diffractograms of pure drug, chitosan and formulation (M1-M4) are given in Figure 5.

### In vitro mucoadhesive strength determination

The *in vitro* mucoadhesion of microspheres was investigated using freshly isolated sheep nasal mucosa [17,18]. The mucosa was obtained from an authorized local abattoir. Within 60 min of slaughtering the animal, the mucosa was excized and fixed still on a plastic support. About 90 mg of microspheres were compressed into a 13 mm disc-shaped tablet which was attached to a coveglass (20 x 20 mm) using cyanoacrylate glue and mounted on the sensor of TRI201 Isometric force transducer (LSI LETICA Scientific Instruments, Panlab S.L., Barcelona, Spain). The test tablet and the mucosal surface were brought into contact in phosphate buffered saline (PBS pH 7.4) at a room temperature. The force required for detachment of the tablet from the lower surface after certain time of contact was measured as a function of displacement, by lifting the glass support at a constant rate of 1  $\text{mm min}^{-1}$  until total separation of the components was achieved. The reported values (Fig. 6) are the average of five different tablets.

### In vitro drug release study

*In vitro* release of BET from the prepared microparticles was studied by diffusion with dialysis bag [19]. The dialysis membrane (Sigma, MWCO 12000 Da) was cut into equal pieces (6 x 2.5 cm) and soaked in distilled water for 24 h before use. An accurately weighed quantity of microparticles (equivalent to 10 mg BET) was suspended in 1 mL of PBS (pH7.4) and placed in the dialysis bag with the two ends fixed by thread. The bag was attached to the paddles of USP type II dissolution tester (AT7 Sotax, Allschwil, Switzerland) and put into 500 mL PBS (pH 7.4) dissolution



medium. The rotation speed was set at 50 rpm and the temperature of the dissolution medium was maintained at  $37 \pm 0.5$  C. Samples of 1 mL were withdrawn from receptor compartment at regular time intervals and replaced with the same amount of fresh PBS. The samples were then analyzed spectrophotometrically as described earlier. The *in vitro* release study was performed in triplicate for each sample. Dissolution profiles of formulation batches M1 - M4 are given in Figure 7.

### Statistical Analysis

All experiments were repeated at least three times. Results are expressed as means  $\pm$  standard deviation (SD). Statistical analysis was carried out employing one-way ANOVA followed by studentized range test using the SPSS Statistics 11.5. A p-value less than 0.05 was considered statistically significant.

## Results and Discussion

### Preparation of the microspheres

The solvent evaporation technique described here appears to be a suitable method for the preparation of chitosan microspheres loaded with BET due to its simplicity, rapidness and reproducibility [20,21]. Four samples of drug-loaded, and corresponding betahistine-free microspheres were prepared using different concentrations of BET and chitosan (1.0%, 1.5% and 2.0% w/v) and varying drug/polymer ratio (1:1, 1:1.5 and 1:2) to investigate modifications of the production yield, particle size, surface topography, drug entrapment efficiency and release behaviour. The

production yield of microspheres was improved from 68.46% to 84.23% when the concentration of the polymer increased (Table 1).

### Drug loading and encapsulation efficiency

BET loaded microspheres were produced with a high drug entrapment efficiency. Higher polymer concentration in the emulsion droplets led to an enhancement of the efficiency of BET entrapment from 69.37 % to 98.27 % (Table 1). Probably, the higher viscosity of chitosan solution tended to restrict diffusion of the drug in the surroundings and enhanced the drug entrapment efficiency [22]. These results indicate very good reproducibility of the solvent evaporation method.

### Optical microscopy

Optical microscopy of BET-loaded microparticles revealed spherical geometry with few aggregates formed in all the preparations. The particle size of each microsphere formulation is reported in Table 1. Mean sizes of the formulations ranged from 3.82 to 7.69  $\mu\text{m}$  which is considered to be appropriate for optimum deposition in the nasal cavity [23]. Increase in chitosan concentration in a fixed volume of aqueous phase resulted in larger particle diameter, which may be due to the fact that the higher the polymer concentration, the higher crosslinking degree. It could be postulated that higher concentration of polymer in the sample led to an enhanced frequency of collisions, resulted in fusion of semiformed particles, and finally increased the size of the microspheres [24]. Photomicrographs of the microspheres are presented in Figure 1.

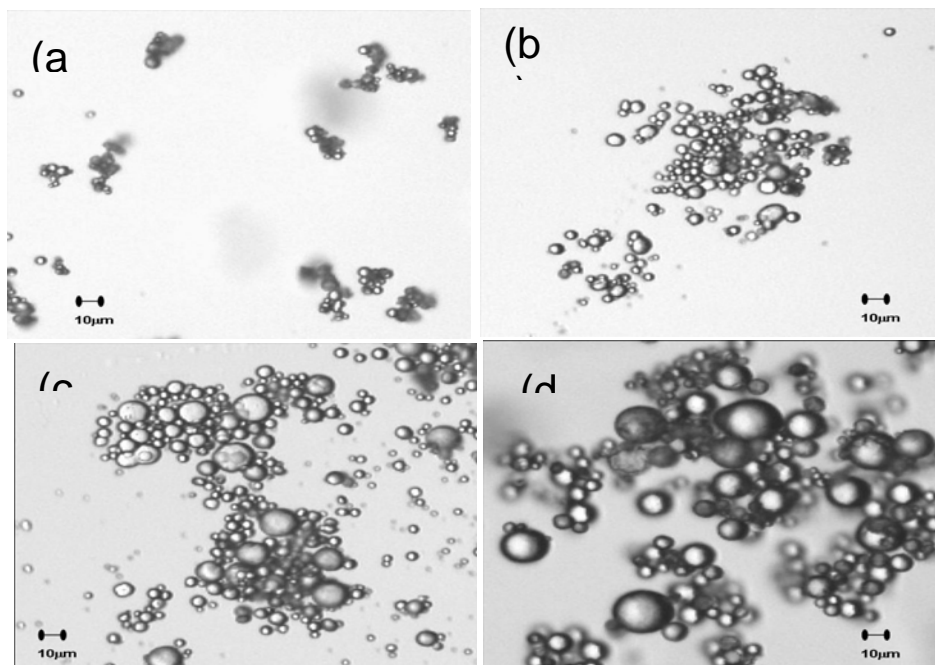


Figure 1. Photomicrographs of BET-loaded microspheres M1(a), M2(b), M3(c) and M4(d) taken at magnification 200x



## Scanning electron microscopy

Studies using SEM provided a better understanding of the morphological characteristics of the microspheres. SEM images of BET-loaded and placebo microspheres are presented at Figures 2(a), 2(b), 2(c) and 2(d), respectively. The placebo chitosan microspheres appeared to have a different morphology when compared to the BET-loaded chitosan microspheres. The placebo microspheres exhibited smooth surface while drug loaded microspheres appeared to have crumpled surface with many wrinkles and gaps between them. The results showed that the

drug/polymer ratio affected the morphological characteristics of the microspheres. As the polymer ratio increased, more furrowed microspheres with larger gaps were obtained. During the solvent elimination process a crust is formed on the outer surface of the droplets. When the inner water phase is evaporated the crust is destroyed, the outer surface collapses and as a result, small pores are formed. The entrapped substance is drained, affecting the loading efficiency. Furthermore, it will concentrate towards the microparticle surface contributing to the initial burst release. Surface hollows could be attributed to the subsequent shrinkage of the microspheres after solidification [25].

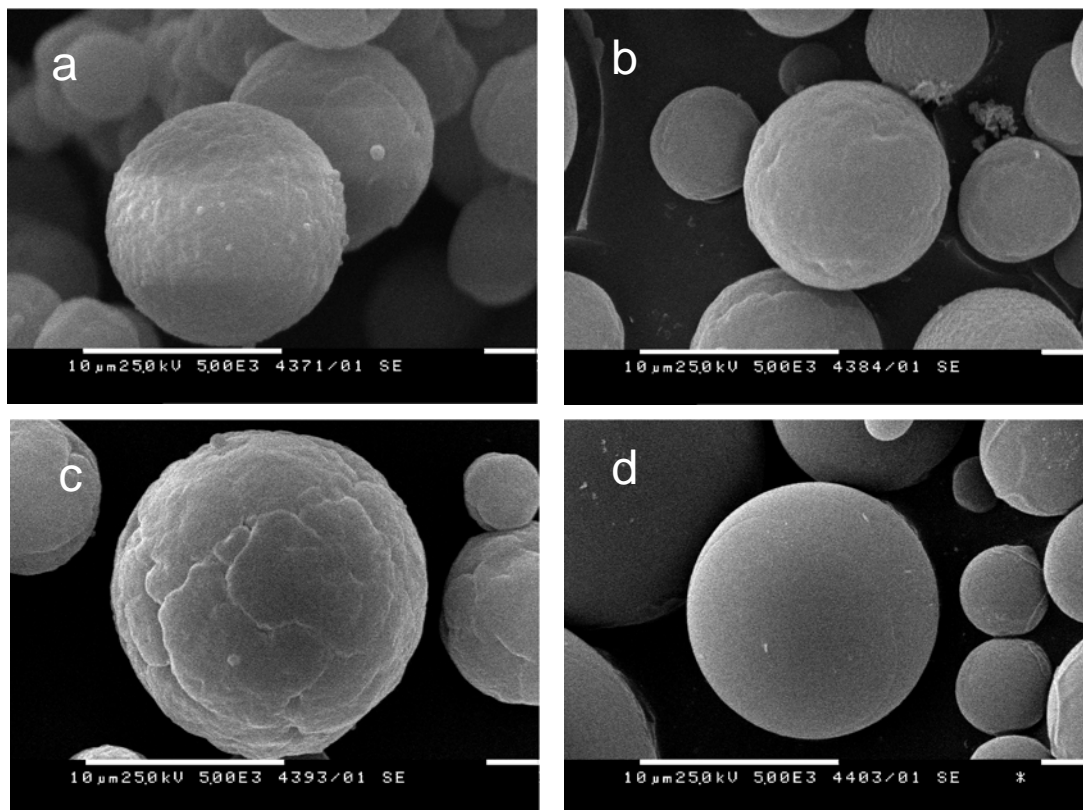


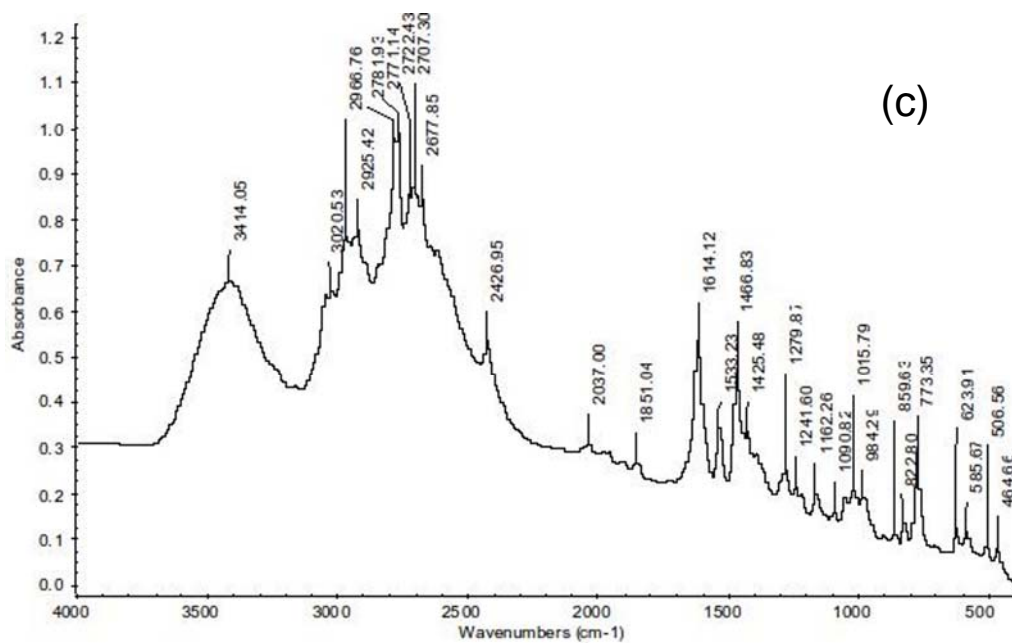
**Figure 2.** SEM micrographs of BET-loaded microspheres of formulations M1(a), M3(b), M4(c) and drug free microspheres (d) at 5000x magnification.

## FTIR spectroscopy

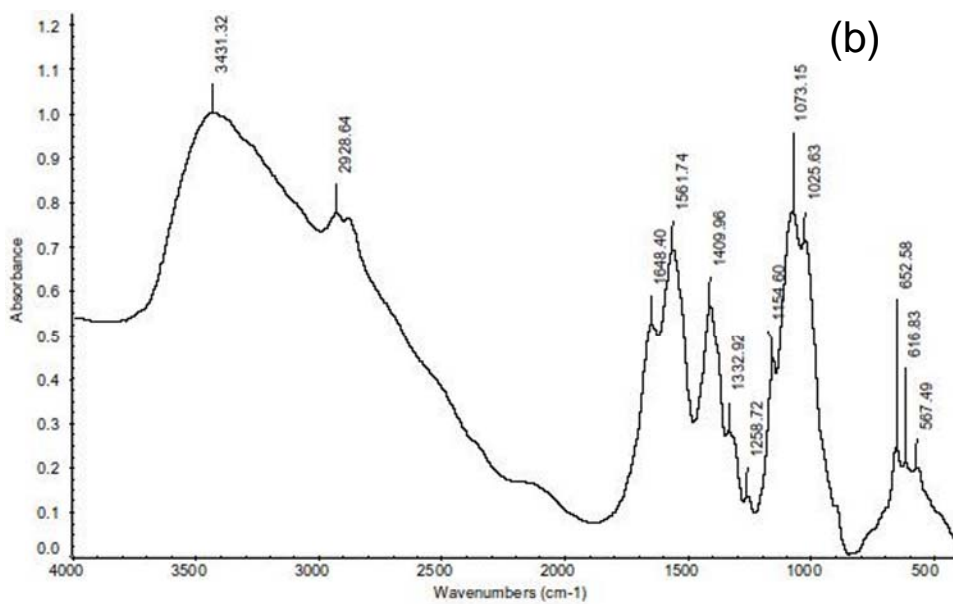
The infrared spectra of BET, chitosan, placebo and drug-loaded formulations are illustrated in Figure 3. BET depicted a broad band at  $3414\text{ cm}^{-1}$ , multiplet at  $3100\text{-}2500\text{ cm}^{-1}$  overlapping absorption of pyridine ring, alkyl groups and ammonium ion ( $\text{R-NH}_2^+$ ) (Fig. 3a). Absorption band at  $773\text{ cm}^{-1}$  is ascribed to  $\gamma$  (out of plane) C-H stretching of 2-substituted pyridines. The spectrum of placebo microspheres (Fig. 3b) shows peaks at  $2928\text{ cm}^{-1}$ ,  $1422\text{ cm}^{-1}$ ,  $1154\text{ cm}^{-1}$  which are attributed to alkyl groups ( $\text{CH}_2$ ). The peaks ranging between  $2700\text{-}3000\text{ cm}^{-1}$  can be ascribed to the stretching of the

$\text{NH}_2$  group with strong overlapping hydroxyl peak between  $3000\text{-}3600\text{ cm}^{-1}$ . Absorption at  $1656\text{ cm}^{-1}$  and  $1597\text{ cm}^{-1}$  is due to  $\text{-CO-NHR}$  group (amide I and amide II) present in the polymeric chain, as a result of the incomplete deacetylation of chitosan. Model systems (Fig. 3c) show broad bands at  $3600\text{-}3100\text{ cm}^{-1}$  and  $3000\text{-}2700\text{ cm}^{-1}$  with increased absorption compared to chitosan. Intensity of all other peaks increases. Absorption peak appears at  $770\text{ cm}^{-1}$  due to BET. No new peaks were observed indicating the lack of new chemical bonds created due to any interaction between BET and chitosan.





(b)



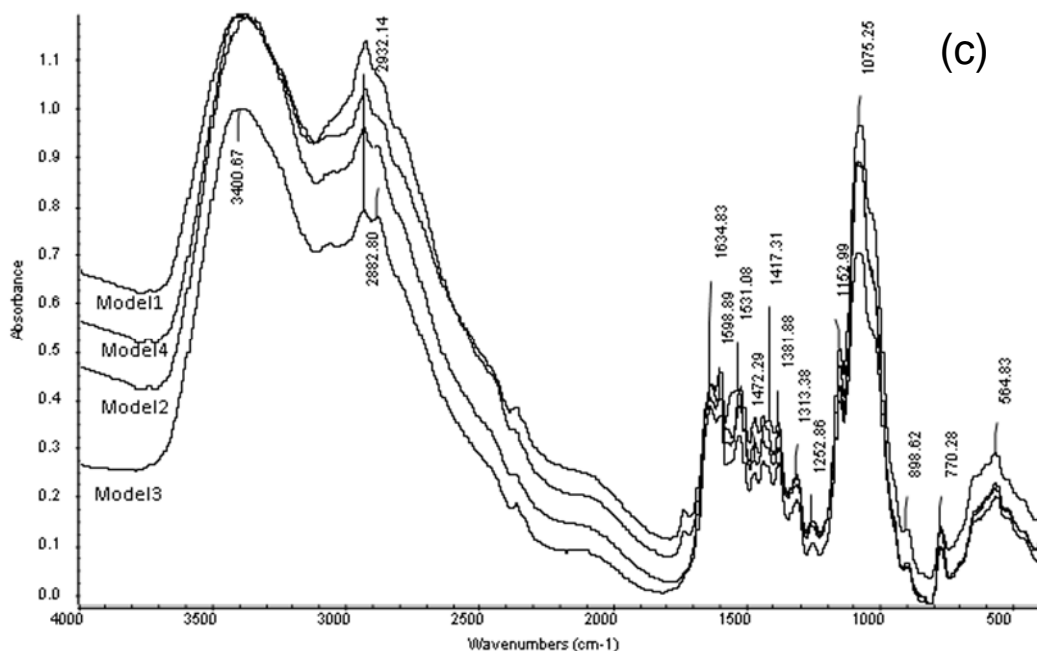


**Figure 3** FTIR spectra of BET (a), placebo microspheres (b) and microsphere formulations (c)

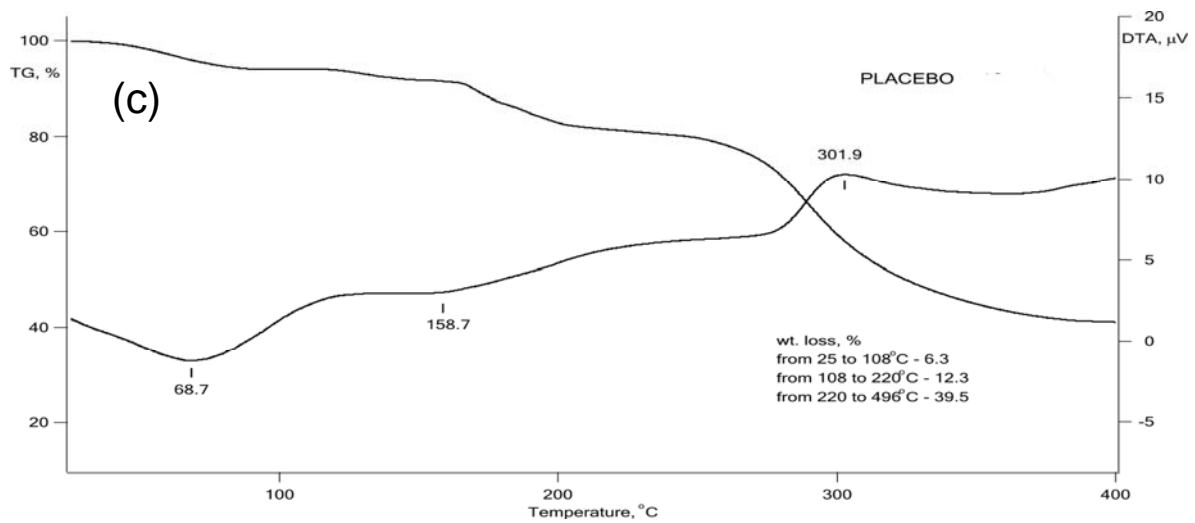
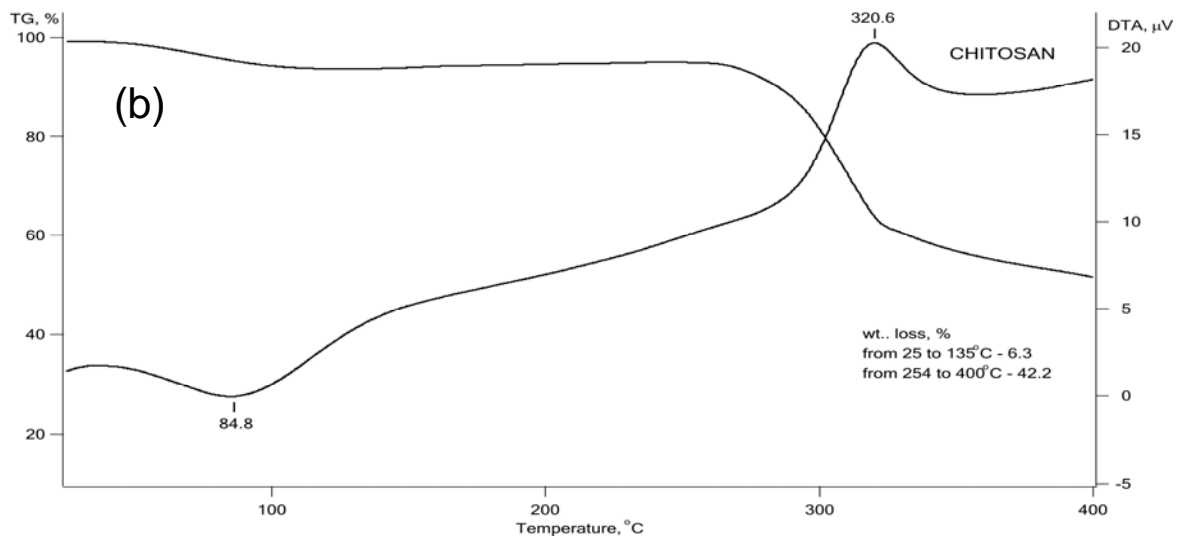
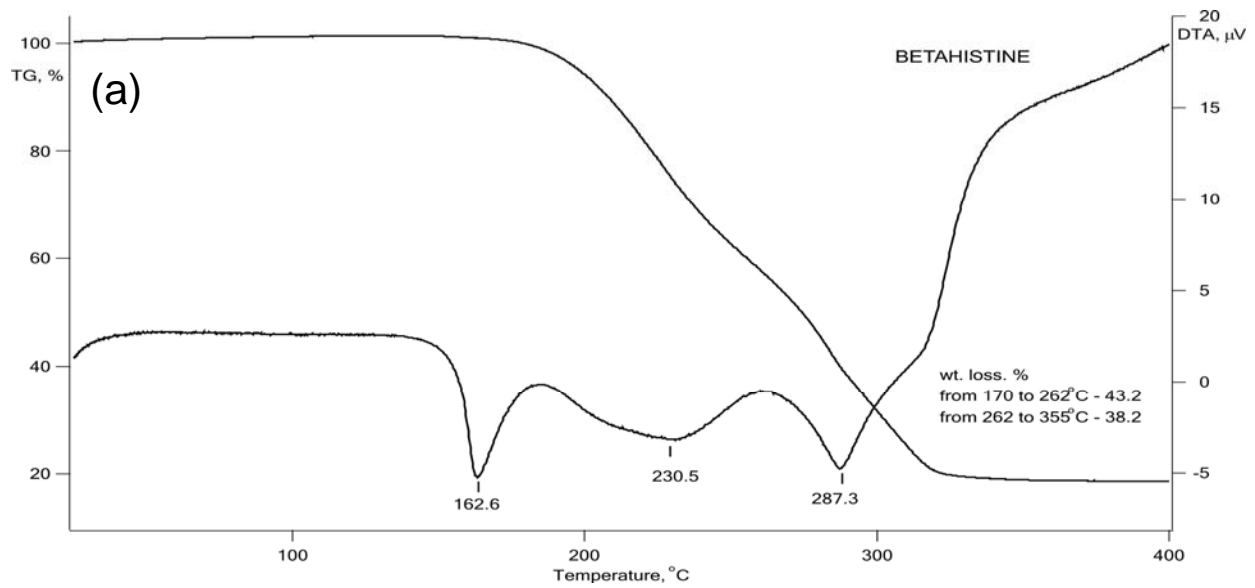
### Thermal analysis

In an effort to assess the physical state of the drug in the chitosan microspheres, we have analysed pure drug, placebo and BET-loaded microspheres using TG-DTA. The thermograms are displayed on Figure 4. The drug (Fig. 4a) presented three endothermic peaks. The first peak is at 162.6 C and corresponds to the melting point. The decomposition process followed the melting of the drug observed as two endothermic effects. As presented at Figure 4 (a), this sharp peak was dramatically reduced in the DTA thermograms of drug-loaded formulations (Fig. 4d). This result suggests that the crystallinity structure of BET was transformed into an amorphous state during the solvent evaporation process and the drug was molecularly dispersed inside the microspheres as supported by X-ray study. Nevertheless BET is hygroscopic in nature and is expected to retain significant amount of water in the microspheres, this was not observed and the endothermic peak assigning water loss from the formulations did not differ from the placebo particles.

Two steps can be observed in the TG-curve of chitosan (Fig. 4b): the first one at about 84 C related to 6.3% weight loss was accompanied by endothermic effect and was attributed to the evaporation of water absorbed in the inner polymer. The second one, beginning at about 250 C and ending at over 400 C was connected with 42.2% weight loss and was indicated for vaporization and burning of volatile compounds produced from the thermal degradation of polymeric chain.

In the DTA curve, a sharp exothermic peak was observed at 320.6 C. According to some authors this event is related to the thermal decomposition of chitosan which occurs in the temperature range 270-337 C due to deacetylation and depolymerization of chitosan. The decomposition temperature of placebo chitosan microspheres was 301.9 C, whereas that of BET-loaded formulations was lower (from 210 to 225 C). Considering the temperature at which thermal degradation starts as a criterion of the thermal stability of microparticulate formulations, it could be seen that the drug/ polymer ratio and BET entrapment influenced the thermal stability of the microspheres with respect to that of plain chitosan [26].







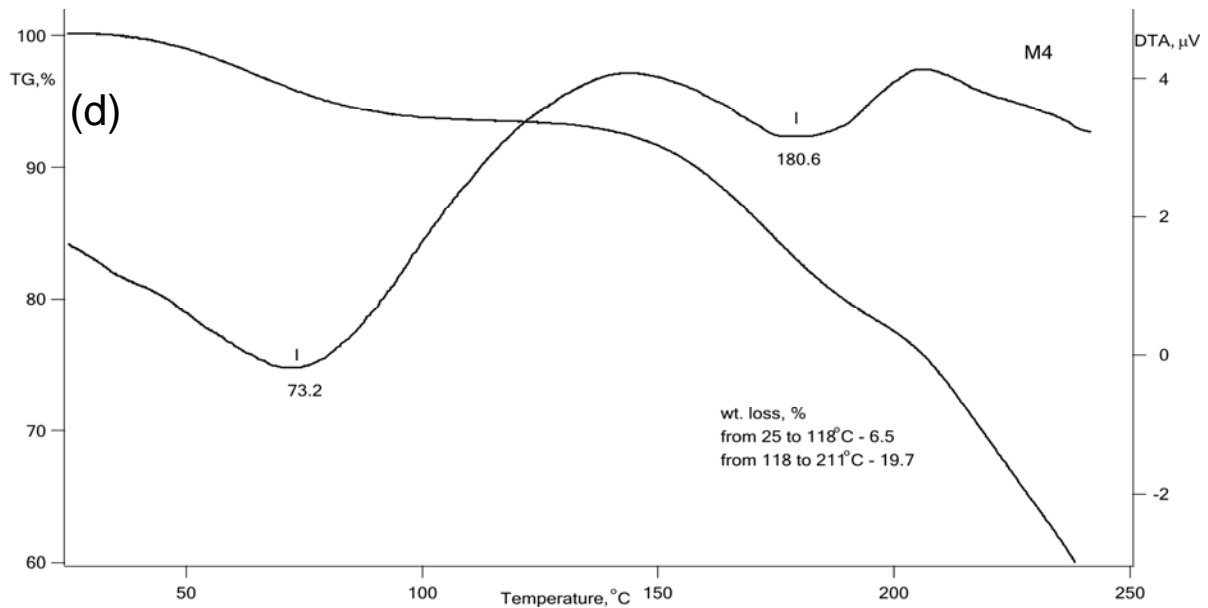


Figure 4. TGA and DTA curves of pure betahistine (a), chitosan (b), placebo microspheres (c) and microsphere formulation M4 (d).

### X-ray diffraction analysis

The X-ray diffractograms of BET, chitosan, placebo and drug-loaded microspheres are shown in Figure 5. The X-ray diffraction pattern for BET displayed the presence of numerous distinct peaks; the diffractogram of pure chitosan powder showed two distinct peaks for the scattering angle  $2\theta$ , equal to  $10.4^\circ$  and  $22^\circ$

approximately while the microparticulate formulations showed one, regardless of drug loading. According to this data BET was crystalline in nature while chitosan was amorphous. The molecular state of BET in the microparticles was changed from crystalline state to amorphous state. This shows that entrapped drug molecule is monomolecular dispersed in the polymer matrix.

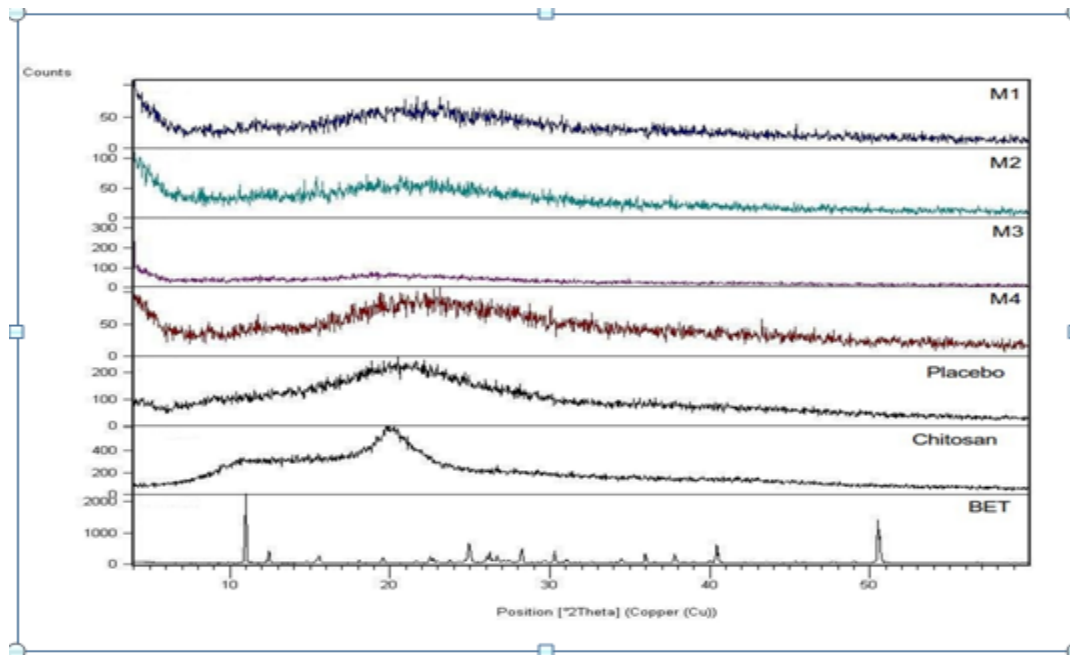
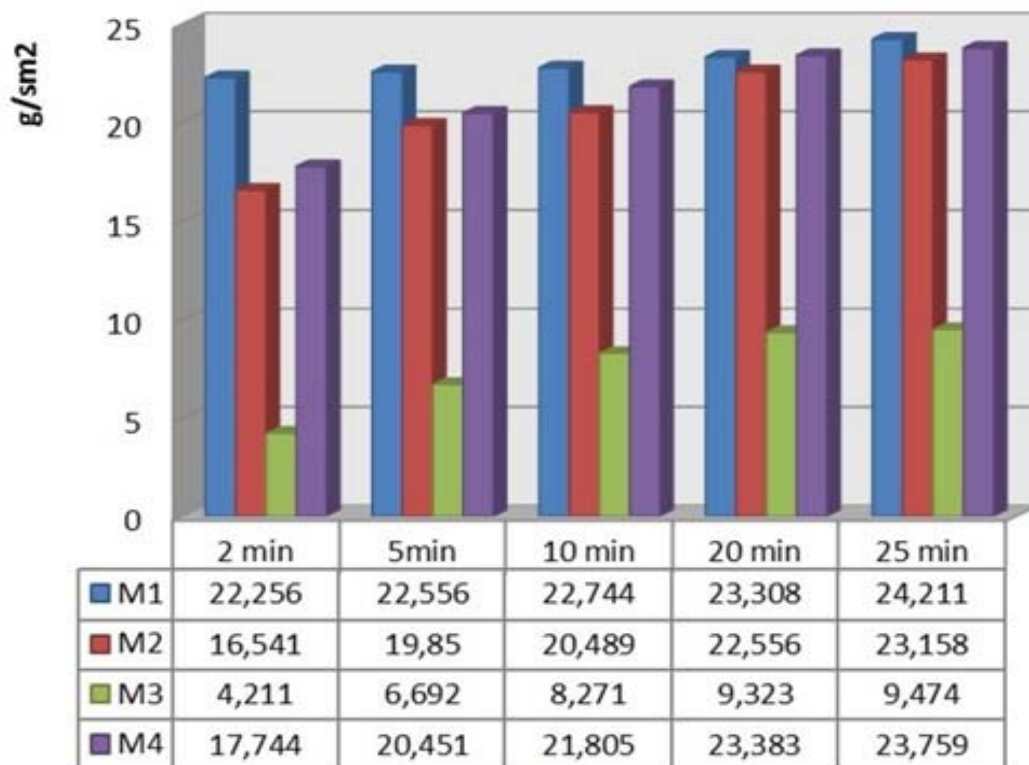


Figure 5. XRD patterns for pure BET, chitosan, blank microspheres (placebo) and drug-loaded formulations (M1-M4).

## In vitro mucoadhesion

In vitro mucoadhesion of the microspheres was the most important aspect of this study. Figure 6 summarizes the results of the tensile studies with BET-loaded formulations on sheep nasal mucosa.



**Figure 6.** Mucoadhesive properties of microsphere formulations M1 – M4 on sheep nasal mucosa. Mucoadhesion was evaluated by tensile studies and is expressed as the detachment force. Indicated values are means of five experiments.

The results showed that all the batches had satisfactory mucoadhesive strength and could adequately adhere to nasal mucosa. Tensile studies performed with BET-loaded microsphere showed that drug/polymer ratio significantly influenced the mucoadhesive properties of the microspheres. Thus, the microspheres with equal BET/chitosan content (1:1, samples M1 and M4) were more adhesive regardless the polymer concentration in the starting solution (1% w/v for M1; 2% w/v for M4). The lowest mucoadhesion was observed with sample M3 (BET/chitosan 1:2) with a clear correlation between the amount of BET in the preparation and decrease in mucoadhesion: the detachment force measured with BET/chitosan ratio 1:2 (sample M3), decreased 5-fold (after 2 min contact time) and 2.5-fold (after 25 min contact) compared to the sample with the highest mucoadhesive strength - M1. This is most likely due to the higher polymer concentration in sample M3. High concentration of polymer imparts larger penetration with maximum adhesion. In few cases beyond optimum concentration, odd effects towards adhesive strength may occur. In highly concentrated systems, the adhesive strength drops significantly. In fact, in concentrated solutions, the coiled molecules become solvent poor and the chains available for interpenetration

are fewer [27]. Another prerequisite for a good mucoadhesion is the high flexibility of polymer backbone structure since it is important for interpenetration and enlargement. The mobility of the individual polymer chain, however, is reduced if the polymer molecules become cross-linked. Chitosan has a flexible, hydrophilic helical structure with reactive amine groups, which offers a multitude of possible inter- and intra-molecular interactions [28]. Lower amount of drug dispersed between polymer chains provides better opportunities for inter-chain conjunction and achieving a higher cross-linking degree. As the cross-linking density increases, the effective length of the chains which can penetrate into the mucus layer decreases. Although highly cross-linked microspheres will absorb water, they are insoluble and will not form a liquid gel on the nasal epithelium but rather a more solid gel-like structure. The highly cross-linked microspheres are more rigid as compared to microspheres with low cross-linking degree and availability of the less number of sites for mucoadhesion, results in reduction in the mucoadhesive properties [29,30]. At the same time, there was no significant difference ( $p>0.05$ ) in mucoadhesion between samples M2 and M4, indicating negligible

influence of drug and polymer concentrations in the starting solutions and drug/polymer ratio lower than 1:1.5.

The initial contact time between microsphere formulations and the mucus layer was investigated as a factor affecting mucoadhesion. The initial contact time determines the extent of swelling and the interpenetration of polymer chains and thus can dramatically affect the performance of the system. Our results show that the mucoadhesive strength is enhanced as the initial contact time increases. No significant difference in the mucoadhesive strength of sample M1 was detected after various time intervals (2, 5, 10, 20, 25 min) presenting excellent mucoadhesive behaviour irrespective of the initial contact time. This was probably due to the smaller particle size of this formulation and the uniform swelling manner of the microspheres. Samples M2 and M4 show uneven particle size distribution and longer time will be needed to achieve equilibrium swelling. These formulations exhibit such mucoadhesive strength after 20 min initial contact time.

### In vitro release studies

The dissolution profiles of BET-loaded formulations are shown in Figure 7. The release of drug from the polymer microparticles was controlled by the formation of a gel which slowed diffusion of the drug across the viscous boundary layer. It is reasonable to suggest that the prolonged release was the result of the gel formation. The percentage of drug release was found to be in the range of 56.08% to 64.98% at a period of 10 hours. Dissolution profiles show that BET was released from the microspheres in a biphasic way with initial rapid drug release (burst effect) from the surfaces of the particles followed by a step of slower release. The initial burst release was probably due to the accumulation of high drug amounts in the periphery of the microspheres during the intense solvent elimination and might be attributed as a desired effect to ensure the initial therapeutic plasma concentrations of drug. The drug in the core of particles is responsible for the prolonged drug release from the polymer matrix. The initial rapid drug leakage generally ended very early (within first 30-60 min); in the remaining time nearly linear behaviour was observed. Two phenomena can attribute to enhancing the diffusion of the remaining dispersed drug into the microspere matrix – formation of pores within the matrix due to the initial drug dissolution and particle wetting and swelling which enhances the polymer permeability to the drug [31]. The release patterns of the samples were similar, with slight differences depending on the formulations drug loading and entrapment efficiency. Sample M1 had the lowest entrapment efficiency (69.37%) and released the smallest percentage of BET. At high loadings, major parts of the drug seem to be located close to the

surface, easily accessible by the release medium. Sample M4 had the highest entrapment efficiency (98.27%) and was expected to release maximum amount of BET. However, our suggestions were not confirmed and sample M4 released smaller amount of BET than M3. This was probably due to the larger particle size of this formulation. Usually, the release of drugs from larger microparticles is slower than that from the smaller ones due to a smaller surface area subject to dissolution [32]. At the end of 10h release of BET was incomplete in all the batches indicating that the chitosan gel layers were too swollen and viscous and hindered the outward transport of core located drug molecules.

To find out the mechanism of drug release, the obtained drug release data were fitted in Korsmeyer-Peppas model. This model is generally used to analyse the release of pharmaceutical polymeric dosage forms, when the release mechanism is not well known or when more than one type of release phenomena could be involved [33]. For these cases, a general equation can be used:

$$M_t / M = Kt^n$$

where  $M_t / M$  is the fraction of drug released at time  $t$ ,  $K$  is kinetic constant incorporating structural and geometric characteristics of the delivery system,  $n$  is the diffusional exponent and is indicator of the mechanism of transport of drug through the polymer. In the case of spherical matrices,  $n = 0.45$  corresponds to a diffusion control (Fickian release),  $0.45 < n < 0.89$  to non-Fickian or anomalous,  $n = 0.89$  to Case II (relaxational) transport, and  $n > 0.89$  super case II transport. For determination of exponent  $n$  the portion of the release curve was used up to  $M_t / M < 0.6$  [34]. The  $n$  values as shown in Table 2 were in the range of 0.1810 to 0.2078 indicating that all the prepared formulations followed the Fickian-diffusion controlled mechanism of drug release.

**Table 2.** Kinetic (Korsmeyer-Peppas model) parameters of BET release from chitosan microspheres

Formulation code	K	R <sup>2</sup>	n
M1	0.3921	0.8348	0.1810
M2	0.3815	0.8335	0.1853
M3	0.3441	0.8680	0.2008
M4	0.3503	0.8889	0.1875

K - kinetic constant; R<sup>2</sup> - coefficient of determination; n - diffusional exponent.



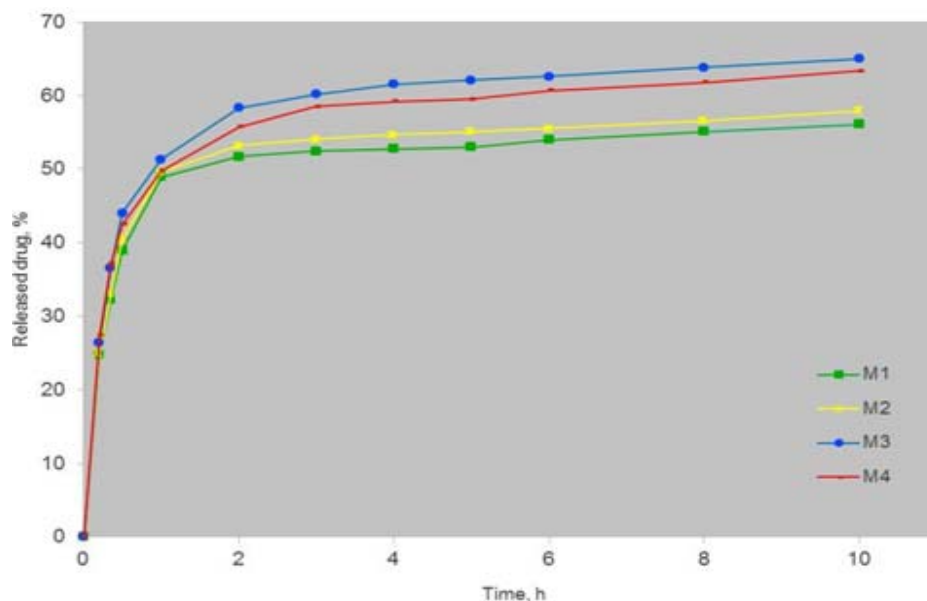


**Figure 7.** Dissolution profiles of BET from microsphere formulations prepared at different drug/polymer ratio. Each data point represents the mean value  $\pm$ SD of three determinations.

## Conclusions

In the present study BET-loaded chitosan microspheres were prepared using emulsion solvent evaporation technique. The microspheres were produced with sufficient production yield and high entrapment efficiency confirming the simplicity and reproducibility of the method described above. The microspheres were at a suitable size and had excellent surface morphology. No chemical reactions were observed between BET and chitosan indicating excellent drug/polymer compatibility. The mucoadhesive properties of the microspheres were strongly influenced by drug/polymer ratio and chitosan concentration had significant effect on BET release rate. The dissolution profiles were similar and slightly increasing when higher concentration of chitosan was used. These results clearly indicate that the chitosan microspheres have

the potential to deliver BET following nasal administration and could be used as a sustained-release drug delivery system.

## Authors' Contributions

BP conceived the study and carried out the microspheres formulation and characterization and drug release study. MK participated in its design and coordination. PZ carried out the mucoadhesion study and performed the statistical analysis. YU carried out the drug-polymer compatibility studies. All authors read and approved the final manuscript.

## Acknowledgements

This study was supported by The Medical University Plovdiv Research Fund according to Intra-university project YS13/2012. The authors declare that there is no conflict of interest.

## References

- [1]. Lacour M, Heyning PH, Novotny M, Tighilet B. Betahistine in the treatment of Ménière's disease. *Neuropsychiatric Disease and Treatment*. 2007;3(4):429–440.
- [2]. Botta L, Mira E, Valli S, Zucca G, Perin P, Benvenuti C, Fossati A, Valli P. Effects of betahistine and of its metabolites on vestibular sensory organs. *Acta Otorhinolaryngol Ital*. 2001;21(3 Suppl 66):24–30.
- [3]. Chávez H, Vega R, Valli P, Mira E, Benvenuti C, Guth PS, Soto E. Action mechanism of betahistine in the vestibular end organs. *Acta Otorhinolaryngol Ital*. 2001;21(3):8-15.
- [4]. Della Pepa C, Guidetti GF, Eandi ML. Betahistine in the treatment of vertiginous syndromes: a meta-analysis. *Acta Otorhinolaryngol Ital* 2006;26:208-215.
- [5]. Williams RO, Taft DR, McConville JT. *Advanced drug formulation design to optimize therapeutic outcomes*. New York: Informa Healthcare; 2008.
- [6]. Alagusundaram M, Chengaiah B, Gnanaprakash K, Ramkanth S, Madhusudhana C, Dhachinamoorthi D. Nasal drug delivery system - an overview. *Int J Res Pharm Sci*. 2010;1(4):454-465.



- [7]. Bitter C, Suter-Zimmermann K, Surber C. Nasal drug delivery in humans. *Curr Probl Dermatol.* 2011;40:20–35.
- [8]. Dhuria SV, Hanson LR, Frey WH. Intranasal delivery to the central nervous system: mechanisms and experimental considerations, *J Pharm Sci.* 2010;99(4):1654-73.
- [9]. Touitou E, Barry BW. Enhancement in drug delivery. Kentucky: Taylor & Francis Inc; 2010.
- [10]. Yadav VK, Gupta AB, Kumar R, Yadav JS, Kumar B. Mucoadhesive polymers: means of improving the mucoadhesive properties of drug delivery system. *J Chem Pharm Res.* 2010;2:418-432.
- [11]. Mathiowitz E. Encyclopedia of Controlled Drug Delivery, Vol. 1 & 2, New York: John Wiley & Sons; 1999.
- [12]. Vasir JK, Tambwekar KR, Garg S. Bioadhesive microspheres as a controlled drug delivery system. *Int J Pharm.* 2003;255:(1-2)13-32.
- [13]. Sinha VR, Singla AK, Wadhawan S, Kaushik R, Kumria R, Bansal K, Dhawan S. Chitosan microspheres as a potential carrier for drugs. *Int J Pharm.* 2004;274:1–33.
- [14]. Patil SB, Sawant KK. Chitosan microspheres as a delivery system for nasal insufflation. *Colloids Surf B Biointerfaces.* 2011;84:384–389.
- [15]. Jadhav KR, Gambhire MN, Shaikh IM, Kadam VJ, Pisal SS. Nasal drug delivery system-factors affecting and applications. *Current Drug Therapy.* 2007;2:27-38.
- [16]. Shaikh RS, Raj Singh TR, Garland MJ, Woolfson AD. Mucoadhesive drug delivery systems. *J Pharm Bioallied Sci.* 2011;3(1):89–100.
- [17]. Davidovich-Pinhas M, Harari O, Bianco-Peled H. Evaluating the mucoadhesive properties of drug delivery systems based on hydrated thiolated alginate. *J Control Release.* 2009; 136:38-44.
- [18]. Tangri P, Khurana S, Satheesh Madhav NV. Mucoadhesive drug delivery: mechanism and method of evaluation. *Int J Pharm & Bio Sci.* 2011;2(1):458-467.
- [19]. Mishra M, Mishra B. Mucoadhesive microparticles as potential carriers in inhalation delivery of doxycycline hyclate: a comparative study. *Acta Pharmaceutica Sinica B.* 2012;2(5):518–526.
- [20]. Parmar H, Bakliwal S, Gujarathi N, Rane B, Pawar S. Different methods of formulation and evaluation of mucoadhesive microsphere. *Int J App Bio Pharm Tech.* 2010;1(3):1157-1167.
- [21]. McGinity JW, O'Donnell PB. Preparation of microspheres by the solvent evaporation technique. *Adv Drug Deliv Rev.* 1997;28(1):25-42.
- [22]. Jyothi NV, Prasanna PM, Sakarkar SN, Prabha KS, Ramaiah PS, Srawan GY. Microencapsulation techniques, factors influencing encapsulation efficiency. *J Microencapsul.* 2009;1(3):1-31.
- [23]. Pereswetoff-Morath L. Microspheres as nasal drug delivery systems. *Adv Drug Deliv Rev.* 1998;29:185–194.
- [24]. Tiwari S, Verma P. Microencapsulation technique by solvent evaporation method (Study of effect of process variables). *Int J of Pharm & Life Sci.* 2011;2(8):998-1005.
- [25]. Rosca IO, Watari F, Uo M. Microparticle formation and its mechanism in single and double emulsion solvent evaporation. *J Control Release.* 2004;99(2):271-80.
- [26]. Georgieva V, Zvezdova D, Vlaev L. Non-isothermal kinetics of thermal degradation of chitosan. *Chem Cent J.* 2012;6(1):81-90.
- [27]. Borade RB, Mahajan YY, Jadhav NP, Kokane JV, Usman MdR, Potdar MB. Bioadhesive multiparticulate (microspheres) drug delivery system: a review. *J Drug Del & Ther.* 2013;3(2):176-185.
- [28]. Morris GA, Castile J, Smith A, Adams GG, Harding SE. Macromolecular conformation of chitosan in dilute solution: A new global hydrodynamic approach, *Carbohydrate Polymers.* 2009;76:616–621.
- [29]. Cunha RA, Soares TA, Rusu VH, Pontes FJS, Franca EF, Lins RD. The molecular structure and conformational dynamics of chitosan polymers: an integrated perspective from experiments and computational simulations. In: Karunaratne DN, editor. *The Complex World of Polysaccharides.* New York: InTech; 2012.
- [30]. Peppas NA, Thomas JB, McGinity JW. Molecular aspects of mucoadhesive carrier development for drug delivery and improved absorption. *J Biomater Sci Polym Ed.* 2009;20(1):1-20.
- [31]. Jelvehgari M, Hassanzadeh D, Kiafar F, Loveymi BD, Amiri S. Preparation and determination of drug-polymer interaction and in-vitro release of mefenamic acid microspheres made of cellulose acetate phthalate and/or ethylcellulose polymers, *Iran J Pharm Res.* 2011;10(3):457-467.
- [32]. Sabyasachi M, Paramita D, Santanu K, Somasree R, Sushomasri M, Biswanath S. Investigation on processing variables for the preparation of fluconazole-loaded ethyl cellulose microspheres by modified multiple emulsion technique. *AAPS PharmSciTech* 2009;10(3):703–715.
- [33]. Costa P, Sousa Lobo JM. Modeling and comparison of dissolution profiles, *Eur J Pharm Sci.* 2001;13(2):123–133.
- [34]. Dash S, Murthy PN, Nath L, Chowdhury P. Kinetic modeling on drug release from controlled drug delivery systems. *Acta Poloniae Pharmaceutica.* 2010; 67( 3):217-223.



